

Article

Voltage Stability and Power Sharing Control of Distributed Generation Units in DC Microgrids

Kafeel Ahmed ^{1,*} , Irfan Hussain ^{1,2}, Mehdi Seyedmahmoudian ¹, Alex Stojcevski ^{1,*} and Saad Mekhilef ^{1,2,3} 

¹ School of Science, Computing and Engineering Technologies, Swinburne University of Technology, Hawthorn, VIC 3122, Australia; ipanhwar@swin.edu.au (I.H.); mseyedmahmoudian@swin.edu.au (M.S.); smekhilef@swin.edu.au (S.M.)

² Power Electronics and Renewable Energy Research Laboratory, Department of Electrical Engineering, University of Malaya, Kuala Lumpur 50603, Malaysia

³ Electrical Engineering Department, College of Engineering, University of Ha'il, Ha'il 81481, Saudi Arabia

* Correspondence: kahmed@swin.edu.au (K.A.); astojcevski@swin.edu.au (A.S.)

Abstract: Advancements in power conversion efficiency and the growing prevalence of DC loads worldwide have underscored the importance of DC microgrids in modern energy systems. Addressing the challenges of power-sharing and voltage stability in these DC microgrids has been a prominent research focus. Sliding mode control (SMC) has demonstrated remarkable performance in various power electronic converter applications. This paper proposes the integration of universal droop control (UDC) with SMC to facilitate distributed energy resource interfacing and power-sharing control in DC microgrids. Compared to traditional Proportional-Integral (PI) control, the proposed control approach exhibits superior dynamic response characteristics. The UDC is strategically incorporated prior to the SMC and establishes limits on voltage variation and maximum power drawn from the DC–DC converters within the microgrid. A dynamic model of the DC–DC converter is developed as the initial stage, focusing on voltage regulation at the DC link through nonlinear control laws tailored for Distributed Generation (DG)-based converters. The UDC ensures voltage stability in the DC microgrid by imposing predetermined power constraints on the DGs. Comparative evaluations, involving different load scenarios, have been conducted to assess the performance of the proposed UDC-based SMC control in comparison to the PI control-based system. The results demonstrate the superior efficiency of the UDC-based SMC control in handling dynamic load changes. Furthermore, a practical test of the proposed controller has been conducted using a hardware prototype of a DC microgrid.

Keywords: DC microgrid; distributed generation; sliding mode control; universal droop control; voltage stability; power sharing



Citation: Ahmed, K.; Hussain, I.; Seyedmahmoudian, M.; Stojcevski, A.; Mekhilef, S. Voltage Stability and Power Sharing Control of Distributed Generation Units in DC Microgrids.

Energies **2023**, *16*, 7038. <https://doi.org/10.3390/en16207038>

Academic Editors: Sreedhar Madichetty and Abdelkader El Kamel

Received: 16 June 2023

Revised: 3 October 2023

Accepted: 6 October 2023

Published: 11 October 2023



Copyright: © 2023 by the authors. Licensee MDPI, Basel, Switzerland. This article is an open access article distributed under the terms and conditions of the Creative Commons Attribution (CC BY) license (<https://creativecommons.org/licenses/by/4.0/>).

1. Introduction

The concept of microgrid (MG) has evolved from a simple network of distributed generation (DG) to a sophisticated, multi-mode-operated network that is automated, self-tuning, capable of trading with the main grid, and capable of isolating faulty components of the system [1]. Direct current (DC) MGs offer several advantages over alternating current (AC) MGs, primarily due to the reduced need for energy conversion systems [2,3]. Most DG sources in MGs, such as fuel cells, photovoltaics, and energy storage, inherently operate on DC, while most load types are also being designed to operate on DC supply, and their dominance is expected to increase in the future [4,5]. The use of DC in MGs helps to minimize the number of conversion steps, thereby reducing energy losses associated with power electronic conversion [6]. Furthermore, high-voltage direct current (HVDC) technology is being explored for efficient interconnection of remotely located MGs and power systems operating at different operational standards [7]. However, the wider deployment

of DC MGs necessitates careful consideration of factors such as voltage stability, protective equipment, safety, and adherence to relevant standards [8–10].

In a DC microgrid (DC MG), various distributed generation (DG) units are connected to a common DC bus using DC–DC converters, as shown in Figure 1. The key objectives for controlling a DC MG are voltage stability and power-sharing among the connected DG units [11–13]. Several methods have been proposed to address voltage instability and ensure equitable power sharing in DC MGs [14–16]. The control of DC–DC converters involves the use of both linear and nonlinear control techniques, such as PWM current or voltage mode control based on proportional–integral (PI) control, hysteresis control, sliding mode control, and others [17–20]. However, traditional control approaches like P, PI, and PID controllers may struggle to handle high-load dynamics [21]. Recently, Hussaini et al. introduced an AI-based hierarchical control scheme to improve DC microgrid current sharing and voltage restoration. This method improves bus voltage management and dynamic performance under varied operating situations while ensuring safety and uninterrupted operation without extra controllers [22]. A comparison of voltage control methods and power sharing methods is summarized in Tables 1 and 2, respectively. Table 1 compares DC microgrid voltage control systems by hierarchy, voltage regulation effectiveness, communication needs, parameter estimation, and control complexity. In Table 2, power-sharing control approaches are compared. Both tables provide a comprehensive overview of DC microgrid control techniques, including their advantages and disadvantages.

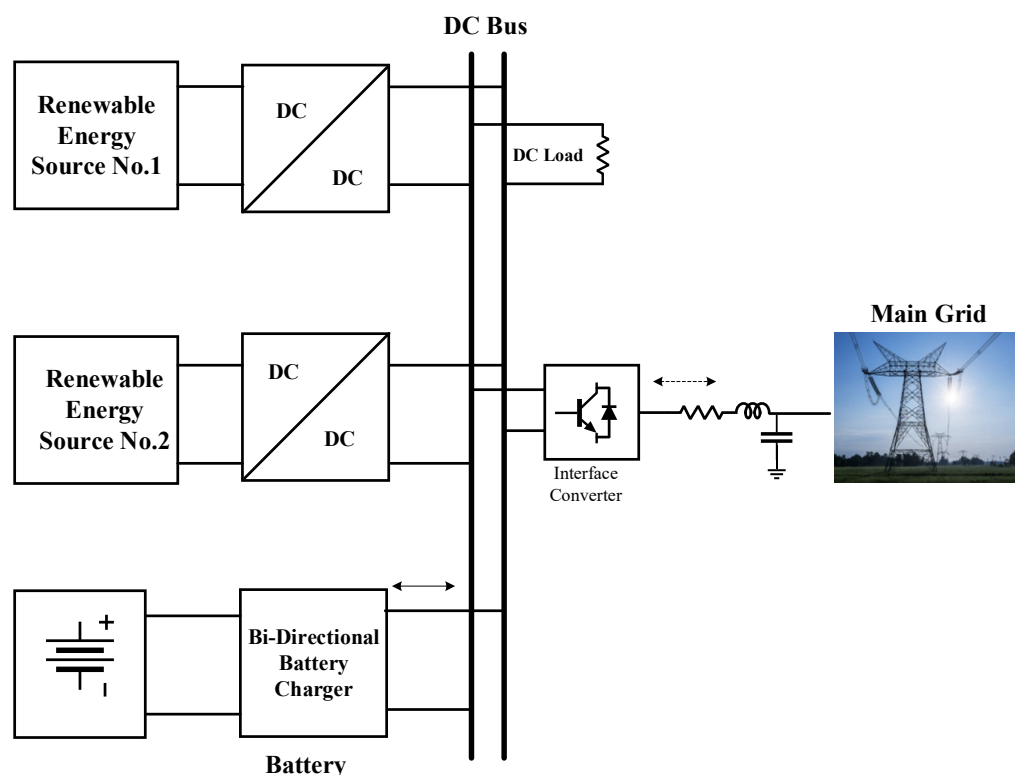


Figure 1. Schematic diagram of a DC microgrid.

Sliding mode control (SMC) has emerged as a promising approach to mitigate voltage deviations during dynamic load changes [2,23]. SMC is based on the principles of variable structure control (VSC) and is renowned for its robustness to parameter variations and disturbances from external sources. It is widely adopted in DC–DC converters due to its inherent robustness and ease of implementation. The design of the sliding mode control (SMC) controller consists of switching states and control laws. In microgrid (MG) control, SMC can be implemented using both fixed-frequency and variable-frequency approaches. However, it is important to note that the frequency is typically kept high,

and the control laws ensure that the controlled parameters oscillate between them at this high frequency. While this high-frequency switching brings robustness to the system, it can also result in power losses due to switching losses, as well as losses in transformers and inductor cores. Moreover, the increased switching frequency can lead to a rise in electromagnetic interference, necessitating careful attention when designing the necessary filters. To address the challenges associated with high-frequency switching, researchers have explored hysteresis modulation-based SMC [20]. This approach utilizes an adaptive hysteresis band and incorporates constant timer circuits to achieve effective control while mitigating the issues caused by the high switching frequency. Combining SMC with other control methods, such as the state space averaging method, the equivalent control approach, and SMC with PWM control, can achieve constant frequency operation. In the case of the equivalent control approach, it is crucial to have a good understanding of the system model and obtain accurate load and input parameters. Adequate knowledge of these parameters is essential for successful control implementation. Another control method investigated in [24] is entirely based on SMC. It utilizes a boost converter model and employs a discontinuous control law to eliminate uncertainties in the model.

Table 1. Voltage control methods.

Control Methods	Hierarchy of Control for Voltage Regulation	Voltage Regulation	Communication	Parameter Estimation Required	Control Complexity
Decentralized control [9]	Secondary control	Very good	Low-bandwidth communication	Yes	Medium
Improved droop control [11]	Primary	Good	Low-bandwidth communication	No	Medium
Feed-forward control [25]	Primary control	Precise	No	No	Low
Virtual resistance control [26]	Secondary control	Very good	Low-bandwidth communication	Yes	Medium

Table 2. Power sharing control methods.

Control Methods	Hierarchy of Control for Voltage Regulation	Power Sharing	Communication	Parameter Estimation Required	Control Complexity
Droop control [12]	Secondary	Good	Yes	No	Medium
Improved droop control [13]	Primary	Good	Yes	No	Low
Virtual negative line resistance [27]	Secondary control	Very good	Yes	No	Medium
Virtual resistance [28]	Primary	Good	Yes	Yes	Low

Model predictive control (MPC) has gained significant attention due to its ability to effectively handle constraints and system nonlinearities [29]. It is particularly well-suited for tracking and regulation problems, offering stabilization properties and high dynamic performance. The working principle of MPC is based on optimization-based tracking, utilizing the system model to anticipate and optimize future behavior. MPC has been extensively employed in the process industry, where system dynamics are typically slow. It holds great potential for power converters due to its fast and dynamic nature. Considering its predictive capabilities and optimization approach, MPC can successfully regulate power converters, accommodating rapid changes and disturbances in the system. However, it requires accurate system modeling to achieve precise performance.

In this paper, we propose a universal droop-integrated sliding mode control (SMC) technique to effectively regulate the voltage of the DC–DC converter and achieve accurate

power sharing among the distributed generators (DGs) in the microgrid. The SMC control offers robustness and adaptability to handle dynamic load variations, load transfers, and power-sharing scenarios. Universal droop control enhances the power-sharing capabilities among the DGs by dynamically adjusting the output power based on the voltage set point and droop coefficient. This integration further improves the performance and stability of the microgrid system, ensuring efficient utilization of the available energy resources. To validate the effectiveness of our proposed control approach, practical implementation is carried out on a testbed. Through extensive simulations and experimental results, we demonstrate the superior performance of universal droop-integrated SMC control over conventional PI control in achieving voltage stability, accurate power sharing, and smooth load shifting in the DC microgrid.

2. Mathematical Model

The microgrid structure considered in this paper, as shown in Figure 2, consists of two voltage-controlled DC–DC converters. These converters, along with their power sources, are hereafter referred to as distributed generation (DG), with one powered by renewable energy (solar PV panels) and the other by battery. Both DGs feed DC loads through a common DC bus. The dynamic model of converters and their control structure is presented below.

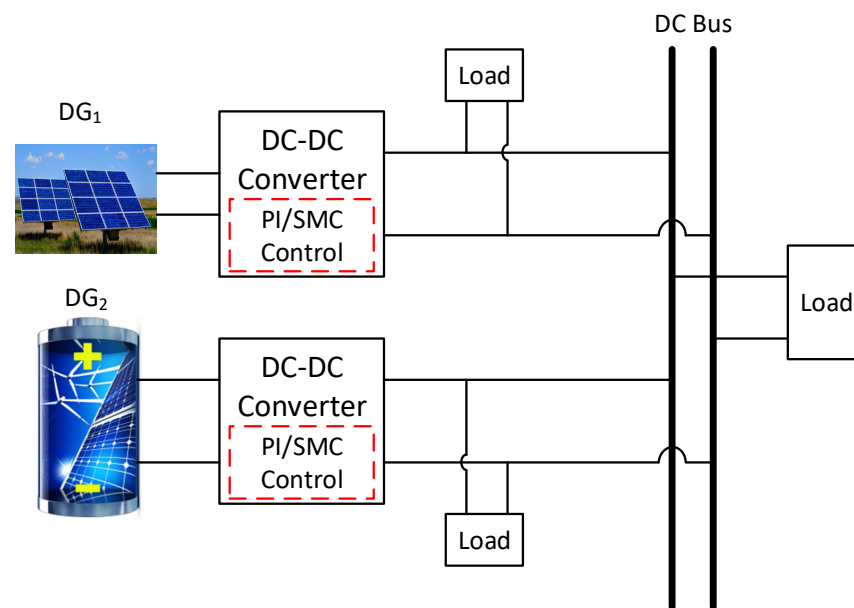


Figure 2. Schematic diagram of DGs connected in a DC microgrid.

Both DG_1 and DG_2 employ a control strategy that combines sliding mode control and universal droop control. This control approach is applied consistently regardless of the different power sources for DG_1 and DG_2 . In this model, we are focusing primarily on implementing the control strategy; therefore, the resistances of the feeders are not taken into account.

2.1. Control of Distributed Generation Units

To evaluate the effectiveness of the proposed control system, despite the heterogeneity in the sources of the distribution generation units, identical DC–DC boost converters have been used to regulate their output voltage. The proposed control system has a hierarchical structure and employs inner and outer control loops. In the outer loop, the universal droop control sets a voltage set point based on characteristics like the droop coefficient and the difference between distributed generation instantaneous power output and its reference.

The outer loop sends this voltage set point to the inner control loop, which directly regulates the DC–DC converters using sliding mode control. The SMC regulates the output voltage despite of variations in the input voltage or the load current.

2.1.1. Sliding Mode Control for DC–DC Converters

Sliding mode control (SMC) is a nonlinear control technique widely known for its robustness against system uncertainties and disturbances. It uses a sliding surface in the system’s state space. The phase in which the control signal first reaches this surface is called the reaching phase. To ensure that the control signal reaches the sliding surface and remains on it during the sliding phase, the control law is established.

The modeling of the DC–DC boost converter in terms of state space and its control parameters is a crucial step. The control of the DC–DC converter in the DC microgrid model is simplified, as shown in Figure 3, to describe the system dynamics. The boost converter switching states and mathematical model representation are given as follows:

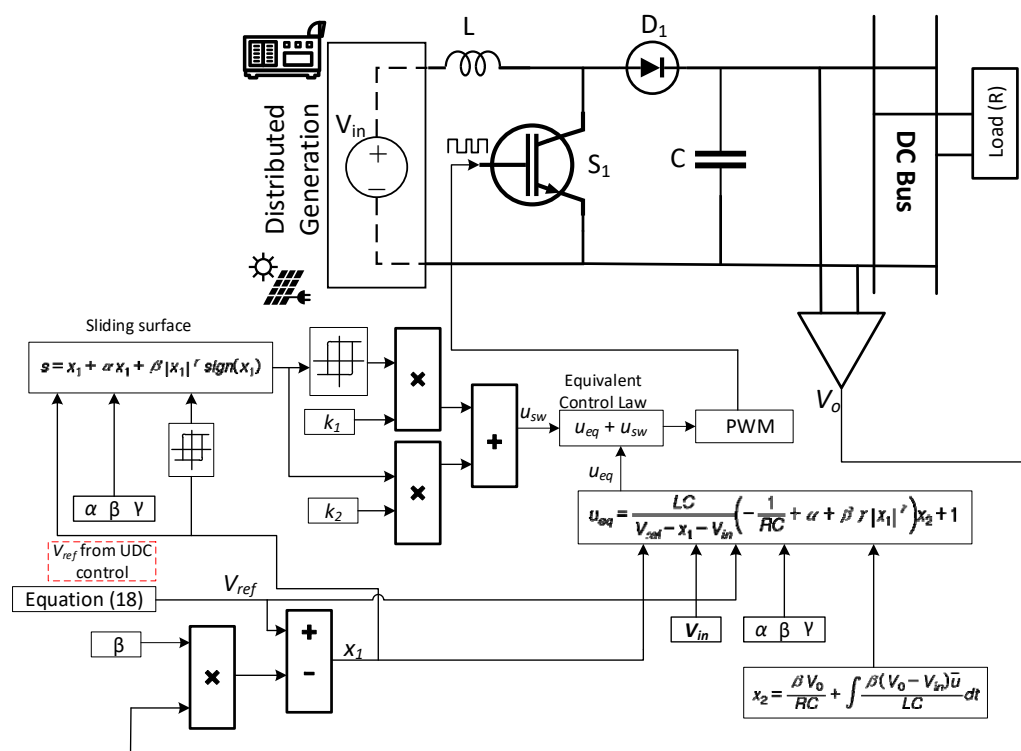


Figure 3. Control of the DC–DC boost converter.

When the controlled switch is closed and the input voltage is applied to the inductor, the inductor current increases as given by Equation (1), and energy is stored in the inductor. Meanwhile, as shown by Equation (2), the capacitor supplies the load and discharges. Switching to the OFF position uses the inductor’s stored energy to power the load and charge the capacitor, as expressed by Equations (3) and (4).

$$\frac{dI_l}{dt} = \frac{V_{in}}{L} \tag{1}$$

$$\frac{dV_0}{dt} = -\frac{V_0}{RC} \tag{2}$$

$$\frac{dV_0}{dt} = \frac{i_l}{C} - \frac{V_0}{RC} \tag{3}$$

$$\frac{dI_l}{dt} = -\frac{V_0}{L} + \frac{V_{in}}{L} \tag{4}$$

L is the inductance, C is the capacitance connected across output terminals, and I_L is the inductor current. The voltage across the load (R) is expressed by the term V . Applying Kirchhoff's current law (KCL) to the capacitor branch node and Kirchhoff's voltage law (KVL) to the inductor loop will define the converter's dynamics depending on the switching function (u).

$$\frac{dV_0}{dt} = (1 - u)\frac{i_l}{C} - \frac{V_0}{RC} \quad (5)$$

$$\frac{dI_l}{dt} = -(1 - u)\frac{V_0}{L} + \frac{V_{in}}{L} \quad (6)$$

where u represents the switching state of the converter switch (1 for the ON state and 0 for the OFF state of the switch).

The dynamic model of the DC–DC boost converter for the SMC control design can be expressed by the following state variables.

$$x_1 = V_{ref} - \beta V_0 \quad (7)$$

$$x_2 = \dot{x}_1 = \frac{\beta V_0}{RC} + \int \frac{\beta(V_0 - V_{in})\bar{u}}{LC} dt \quad (8)$$

where V_{ref} is the reference for the output voltage, x_1 and x_2 represent the voltage error and the voltage error dynamics (or the rate of change of voltage error), β is the feedback network ratio, and \bar{u} represents the inverse logic of u . The above equations can be combined to devise the dynamic model of DC–DC boost converter control, which is represented as

$$\dot{x}_2 = -\frac{x_2}{RC} - \frac{x_1}{LC}\bar{u} + \frac{(V_{ref} - V_{in})}{LC}\bar{u} \quad (9)$$

The following expression describes the switching surface. The reason for this selection is to make sure that the voltage error, which is shown by x_1 , approaches zero at a certain rate and stays on the sliding surface during the operation. The parameters α , β , and γ determine the shape and behavior of the sliding surface.

$$s = x_1 + \alpha x_1 + \beta|x_1|^\gamma \text{sign}(x_1) \quad (10)$$

It must comply with the Routh–Hurwitz rule for achieving stability, i.e., sliding coefficient $\alpha > 0$ and $0 < \gamma < 1$. For which the control law for reaching mode can be presented as

$$u = \frac{1}{2}(1 + \text{sign}(s)) = \begin{cases} 0 & s < 0 \\ 1 & s > 0 \end{cases} \quad (11)$$

The control law (11) implies that the switch should be closed ($u = 1$) when the voltage error x_1 is positive, and the switch should be open ($u = 0$) when the voltage error x_1 is negative. The path of the control signal lies within the boundary defined by the sliding surface and is presented as

$$0 < \left(\frac{1}{RC} - \alpha - \beta\gamma|x_1|^{\gamma-1}\right)x_2 < \frac{V_{ref} - V_{in}}{LC} - \frac{x_1}{LC} \quad (12)$$

The equivalent control function is

$$u_{eq} = \frac{LC}{V_{ref} - x_1 - V_{in}} \left(-\frac{1}{RC} + \alpha + \beta\gamma|x_1|^{\gamma-1}\right)x_2 + 1 \quad (13)$$

A supplementary exponential has been presented in place of reaching the law with a constant rate to stabilize the controller from any preliminary conditions, and it is expressed as

$$u_{sw} = k_1 \cdot \text{sign}(s) + k_2 \cdot s \quad (14)$$

Considering k_1 and k_2 are higher than zero, the cumulative control law is presented as

$$u = u_{eq} + u_{sw} \quad (15)$$

Lyapunov stability is applied to check the effectiveness of the controller, and it is presented as

$$V(t) = \left(\left(-\frac{(V_{ref} - x_1 - V_{in})}{LC} \right) (k_1 \cdot \text{sign}(s) + k_2 \cdot s) + d(t) \right) \quad (16)$$

where $V(t)$ is the Lyapunov function, and the above relation indicates that if the system uncertainties and disturbances, represented by $d(t)$, are bound in such a way that

$$|d(t)| < \frac{V_0 - V_{in}}{LC} (k_1 + k_2) \quad (17)$$

the derivative of the Lyapunov function will be negative-definite if the stability condition in Equation (17) is met, indicating that it decreases over time, primarily because the values of k_1 and k_2 are consistently large, positive, and definite. This shows that the implementation of a control signal for sliding mode control (SMC) ensures that the tracked error converges to zero within a finite time frame.

2.1.2. Universal Droop Control

Droop control is frequently used in AC and DC microgrids to regulate power sharing among the parallel DGs. The primary advantage of droop control is that it does not require any communication network between the DGs. It does not link to any centralized controller and utilizes local measurements only. By implementing droop control, the DC–DC converter will adjust its output voltage in response to changes in load current. This can help maintain a more stable and balanced operation within the microgrid.

With the proposed universal droop control (UDC), the reference voltage for each DG is determined by the provided reference power (P_{ref}), droop coefficient (m), and the measured output power (P) and voltage of the DG. As the output power of the DG varies, the droop coefficient causes the output voltage to adjust. As the power consumption from the DG rises, its output voltage declines. The integration of UDC into DC–DC converter control is depicted in Figure 4.

$$V_{ref} = V_o - m(P_{ref} - P) \quad (18)$$

where V_{ref} is the reference for the DC bus voltage calculated by the UDC loop and fed to the SMC control as reference voltage, and V_o is the output voltage across the DC bus. Equation (19), which describes the droop coefficient, is defined as

$$m = \frac{\Delta V}{P_{max}} \quad (19)$$

ΔV is an allowable limit for the change in voltage, and P_{max} is the maximum power rating of the DG. The output power depends on output voltage and droop coefficient, as shown by the droop curves presented for various droop coefficients (m_1, m_2, \dots, m_n) in Figure 5. As more power is drawn from the DG, the voltage decreases following the slope defined by the droop coefficient. This voltage reduction helps to maintain a balance in power sharing among multiple DGs in a microgrid. When the load increases, causing an increase in power demand, the DG will adjust its output voltage accordingly to provide the

required power. Droop control is an approach to ensuring that DGs share power based on their output power levels.

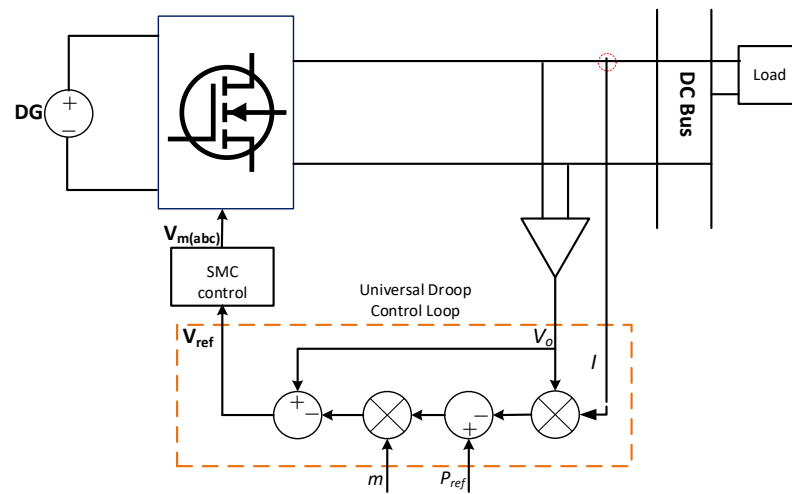


Figure 4. Universal droop control of a distributed generation unit.

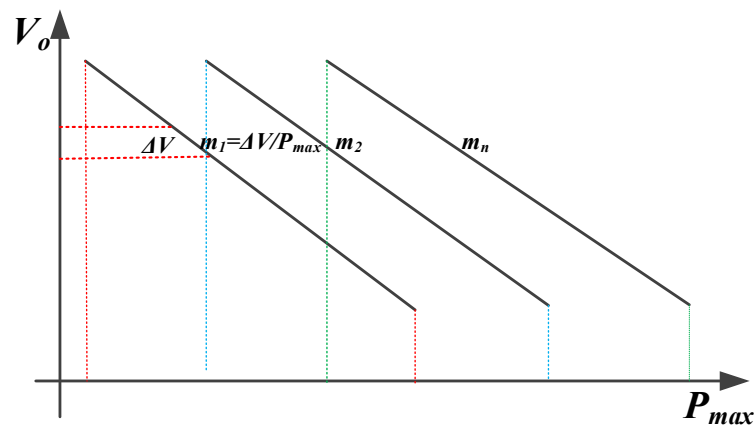


Figure 5. Droop curves for various droop coefficients.

3. Simulation of Proposed Control System and Results

The performance of the proposed control system has been evaluated by modeling the system in PSIM 2022.1 simulation software. Table 3 provides a list of the system specifications and controller parameters. To evaluate the effectiveness of the proposed sliding mode control (SMC) technique, simulations were conducted on a microgrid model represented in Figure 2. Multiple loading conditions were applied, including dynamic load changes, load transfer, and power sharing, with the aim of examining voltage stability, precise power sharing, and seamless load shifting.

Table 3. Simulation parameters for the control of DC–DC converters.

Parameters	Values
DC source voltage (input voltage)	$V_{in} = 96 \text{ V}$
Output voltage	$V_o = 200 \text{ V}$
Beta	$\beta = 1/6$
LC values	$C = 220 \text{ }\mu\text{F}, L = 450 \text{ }\mu\text{H}$
Switching frequency	50 kHz
Droop coefficient	$m = 0.02$
Proportional gain	$K_p = 0.382$
Integral gain	$K_I = 0.0127$

3.1. Steady-State Analysis

The proposed control system employs a combination of sliding mode control (SMC) and universal droop control (UDC) techniques to independently regulate multiple distributed generators (DGs) within a microgrid that share a common DC bus. Control actions are determined within each DG controller based on local data, without the need for communication between DGs. To achieve power-sharing among the DGs, universal droop control is implemented at a higher hierarchical level. To evaluate the performance of the proposed control, the same MG model is also implemented with a PI controller, and the results are then compared. Figure 6 illustrates the output voltage, current, and power distributed among each DG unit under both control methods. The results indicate steady and reliable performance with regard to maintaining a stable voltage and distributing power evenly. However, it is worth noting that with a PI controller, the settling time of the voltage signal is 30 ms, which is higher as compared to the proposed control.

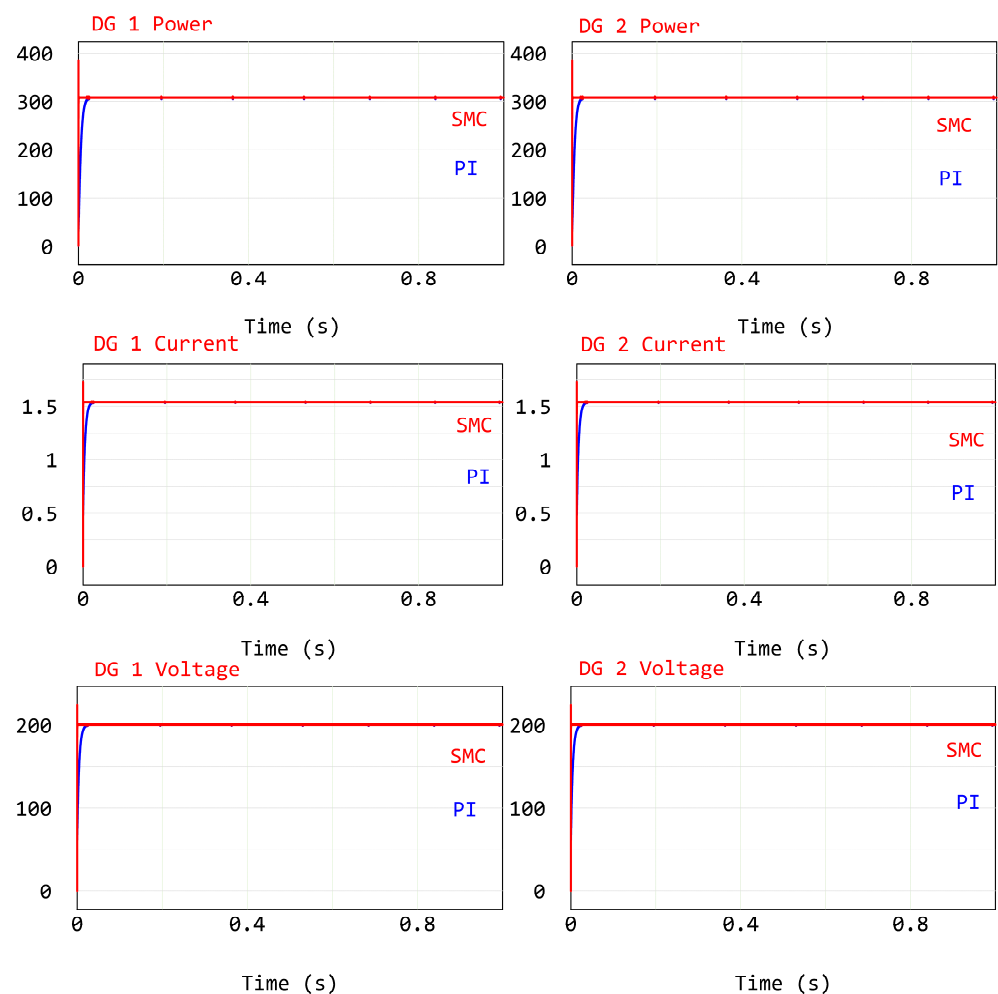


Figure 6. Output voltage and load current of a PI controller in the steady-state condition.

3.2. Transient State Analysis

The robustness of the individual control technique can be assessed by conducting tests involving dynamic load changes and hot-swap operations. These tests serve to evaluate the ability of the control technique to adapt and maintain stable performance in the case of varying load conditions and the failure of a particular DG.

3.2.1. Study I: Dynamic Load Changes

Figure 7 illustrates the performance of the SMC and PI techniques in terms of dynamic stability. To evaluate how they respond to shifts in power demands, step changes are applied to power references across DGs for both control methods at 0.5 s. The power reference of DG 1 is doubled, and its power is increased from 300 W to 600 W, while DG 2's power reference is decreased from 600 W to 300 W. During this brief period, the current rises to augment DG 1's output power, leading to a minor dip in the output voltage, which quickly settles within a few milliseconds. Similarly, when DG 2's output power sharply decreases, it results in an increase in the output voltage at DG 2's terminals. After the transient period, both DGs exhibit stable output current and voltage at their terminals, effectively sharing power, according to the provided references.

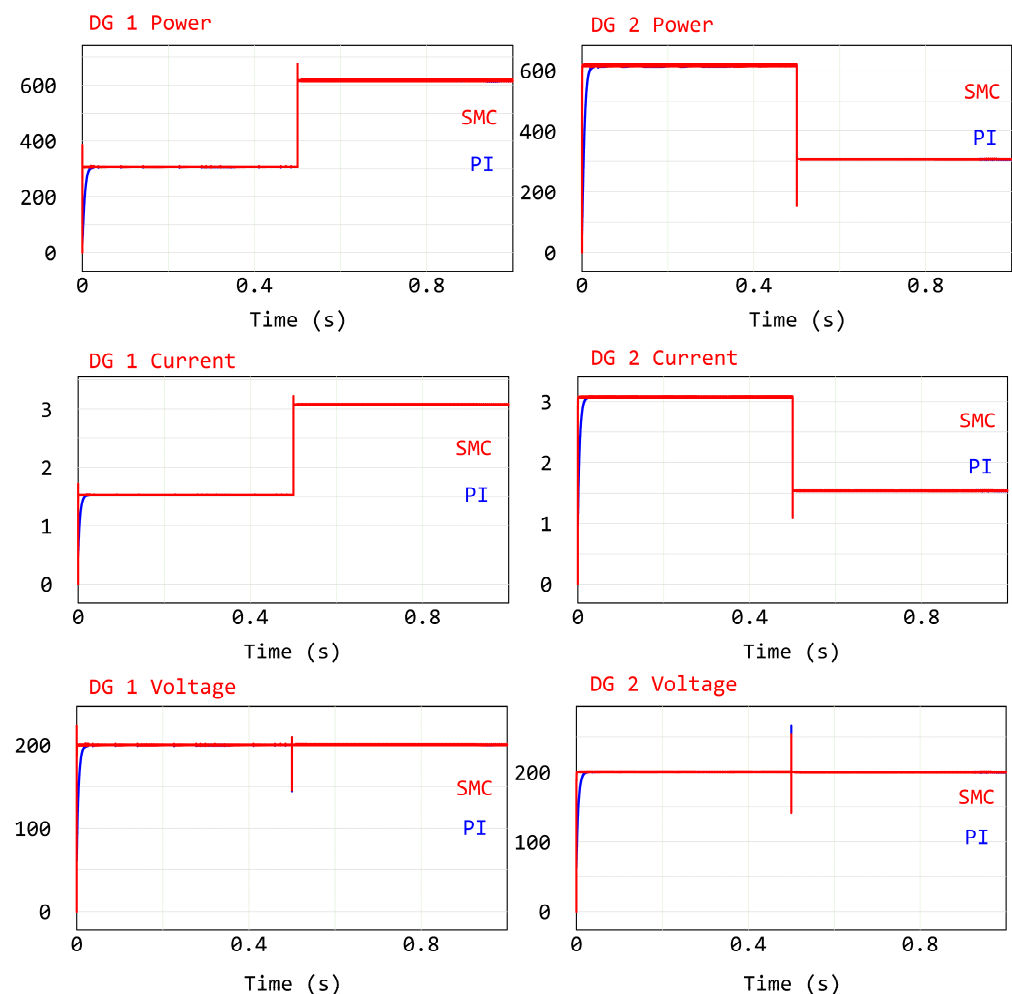


Figure 7. Dynamic response of DG₁ and DG₂ under SMC and PI controllers in transient states.

3.2.2. Study II: Load Shifting

To evaluate the performance of UDC-integrated SMC control, a hot-swap operation was conducted on a DC microgrid model. During this test, we switched the loads between DG 1 and DG 2. DG 1 initially fed all the load, and DG 2 was disconnected from the microgrid. At 0.5 s, DG 1 detached from the MG, and DG 2 took over the full load. During this transition, the current of DG 1 dropped to zero, while DG 2 increased its output current to match the full load. The output results of the DG units using the proposed control and PI control are depicted in Figure 8.

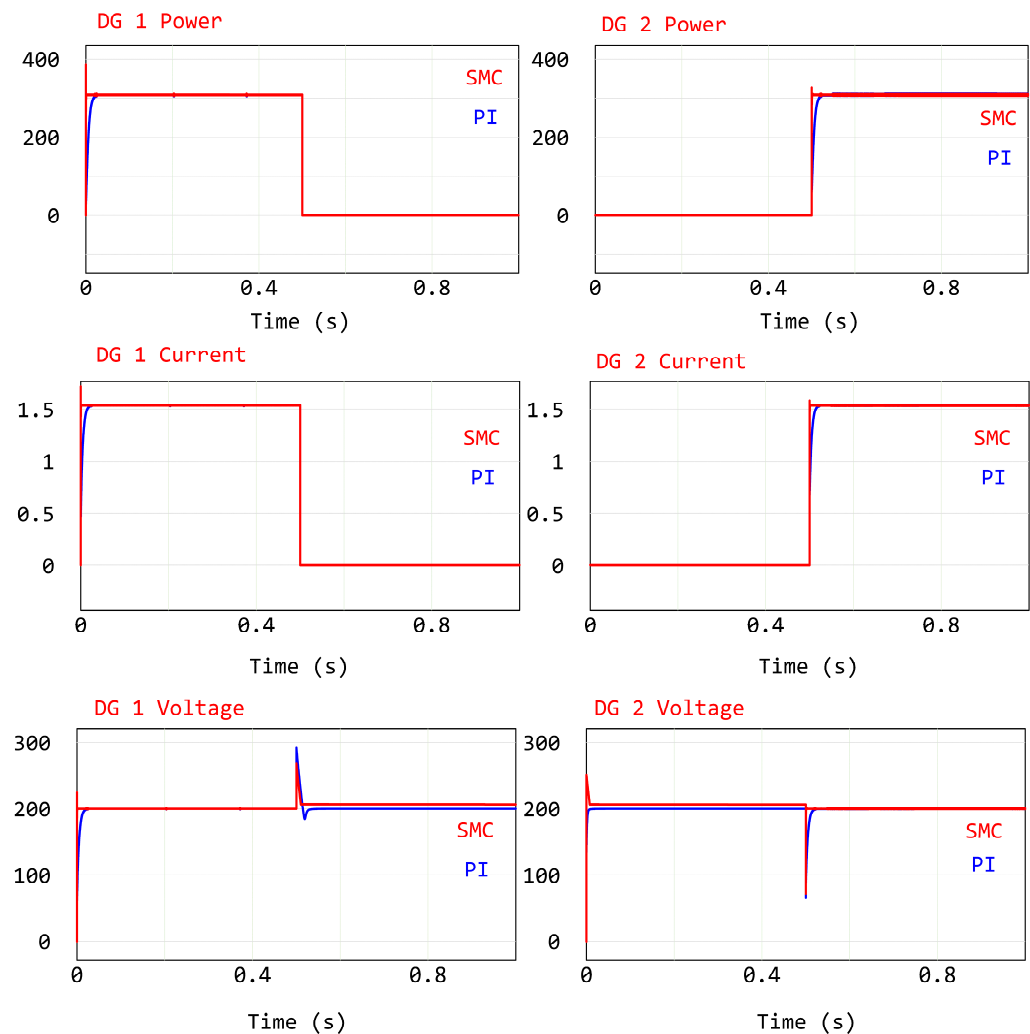


Figure 8. Dynamic response of output parameters DG_1 and DG_2 under SMC and PI controllers during hot-swap operation.

During the hot-swap operation, both control techniques demonstrated stable voltage and current quality. The transition time was characterized by smooth load transfers from one DG to another. However, it is worth noting that the transient time of the PI control was slightly longer compared to the proposed control, which highlights the suitability of the proposed control technique for dynamic load scenarios.

The converters are designed to operate at an output voltage of 200 V. They were tested under both minimum load (20Ω) and maximum load (200Ω) conditions, with step changes in the load. During these load changes, the output voltage requires some time to settle. However, when employing the proposed SMC control, the output voltage remains nearly constant within the specified range of load changes. Table 4 presents the voltage deviation observed with the proposed control, which is only 1.1 V, significantly lower than the deviation observed with the PI control. In the case of the PI controller, the voltage deviates by 1.88% from the nominal voltage, whereas the deviation remains negligible with the SMC control. This comparison highlights the superior robustness of SMC over PI control in handling dynamic loads.

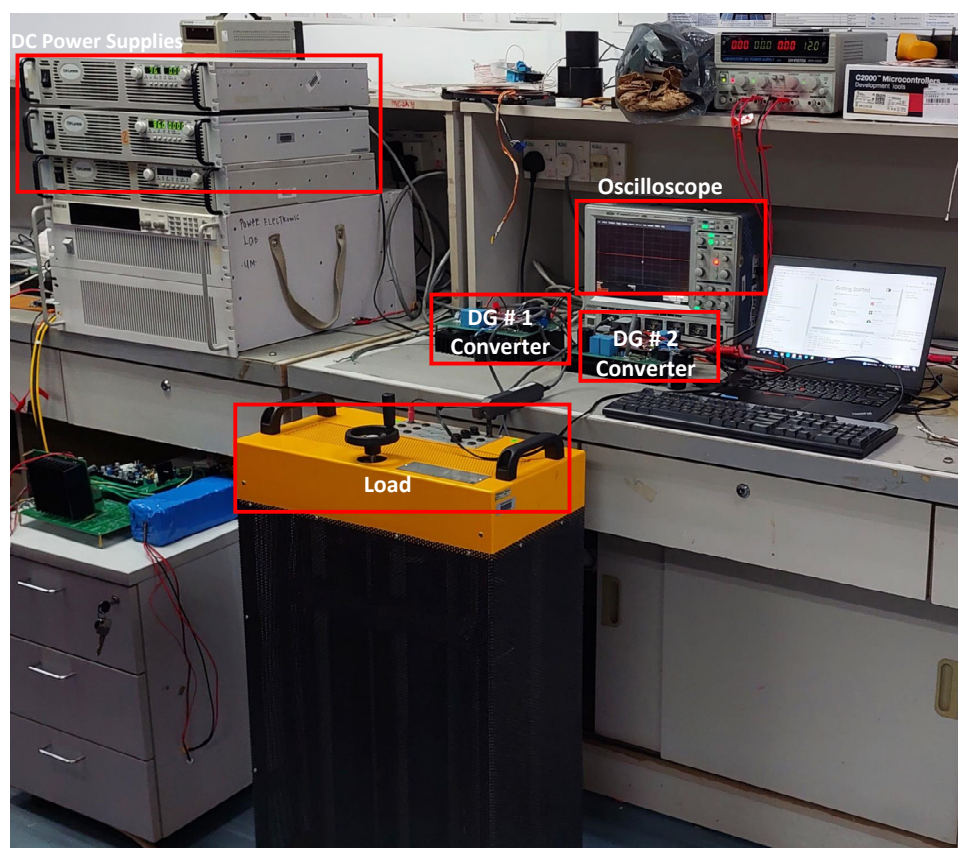
Table 4. Load regulation of SMC and PI for minimum and maximum load conditions.

Control Technique	Voltage Deviation: $\Delta V = V_o(200 \Omega) - V_o(20 \Omega)$	Percentage Change: $(\Delta V_o)/V_o(\text{nominal}) \times 100\%$
PI	3.76 V	1.88%
SMC	1.1 V	0.5%

4. Experimental Set-Up and Results

4.1. Experimental Set-Up

The evaluation of the proposed control has been conducted using a laboratory-scale DC microgrid (MG) testbed. The testbed configuration, shown in Figure 9, comprises two parallel boost converters rated at 400 W each, with each converter being independently managed by the proposed control. Separate DC power supplies are used to provide power to both converters. To assess the real-time performance of the proposed control, Launchpads MCU F28379D, equipped with a TMS320F28379D dual-core high-frequency processor operating at 200 MHz, are employed. The launchpads are directly connected to PSIM using TI C2000 Delfino assistance from the embedded coder. Each DC–DC converter’s associated proposed control is burned onto a separate launchpad, with a switching frequency set at 50 kHz. The PWM output ports of each Launchpad are linked to the GPIO port connected to the system. For testing purposes, a TERCO resistive load is utilized to simulate various loading conditions, allowing for the evaluation of the controller’s performance under dynamic load changes, load transfer, voltage stability, accurate power sharing, and smooth load shifting. Transducers LV 25-P and LAH 25-NP are employed to measure the output voltages and currents, respectively.

**Figure 9.** Experimental set-up of a DC microgrid.

4.1.1. Steady-State Analysis

A load of 500 watts is evenly shared between the two converters by setting their power references accordingly. The proposed SMC control for each converter operates independently, but both are provided with the same power reference, ensuring equal power sharing. This balanced power distribution is clearly depicted in the experimental results presented in Figure 10. The output of each DG converter is measured to be approximately 250 watts, with each DG supplying 1.3 A of current while maintaining a stable voltage of 200 V at the DC bus.

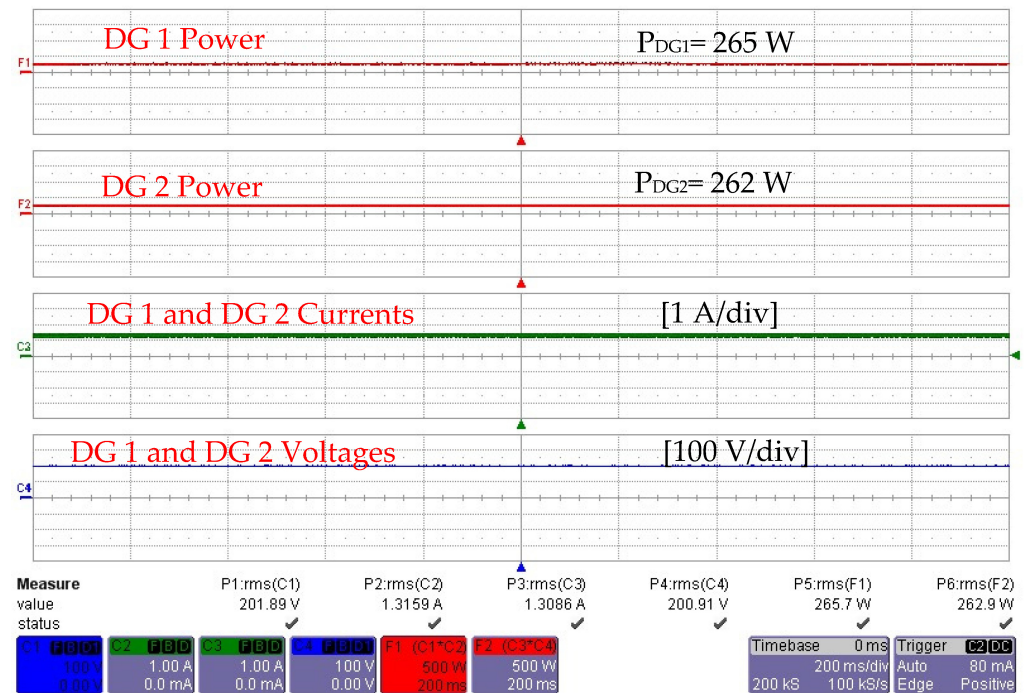


Figure 10. Steady-state response of DG units.

4.1.2. Transient State Analysis

The robustness of the individual control technique can be evaluated when it is investigated for dynamic load changes and hot-swap operation.

Study I: Load Dynamics

Step changes are applied to the power references of both converters to evaluate their performance under dynamic load conditions at different time intervals. Initially, the power reference of the DG 1 converter is doubled, while the power reference of the DG 2 converter is halved. Subsequently, a reverse step change occurs, where the power reference of DG 1 is halved and the power reference of DG 2 is doubled. As a result of these power reference changes, the current and power of each converter vary accordingly. Figures 11 and 12 illustrate the current and power profiles of both DGs, showcasing the impact of step changes in power references at different time instances while maintaining a stable voltage across the DC bus.

Throughout these tests, smooth operation was observed, and despite minor deviations in the currents during these dynamic transitions, the controller quickly and effectively adjusted the output voltage to ensure stability.

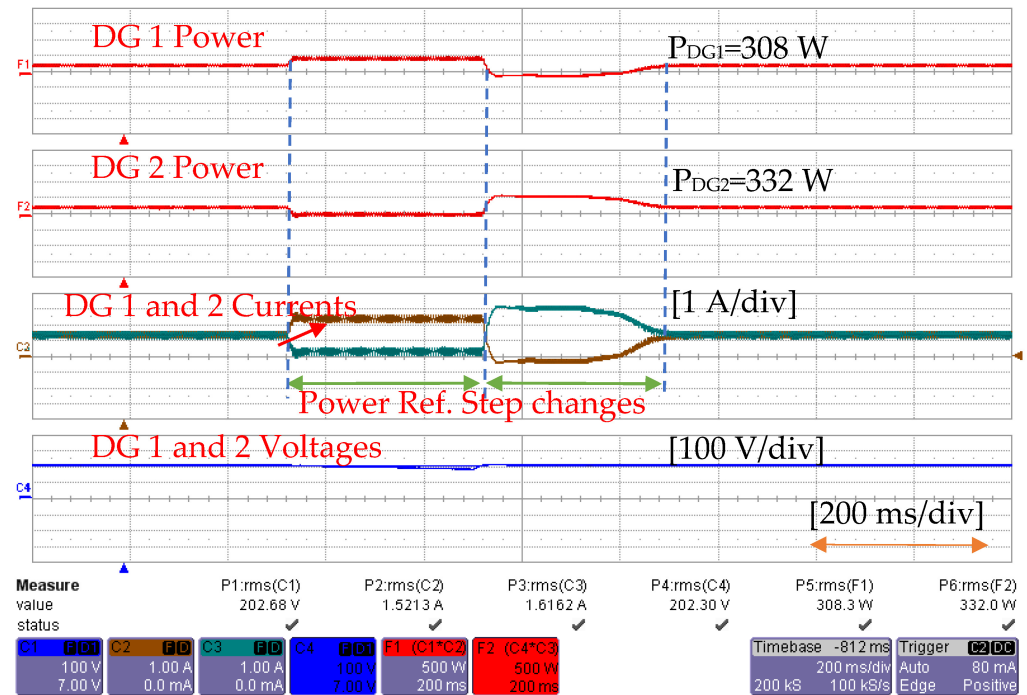


Figure 11. Dynamic response of DGs output parameters with proposed SMC control.

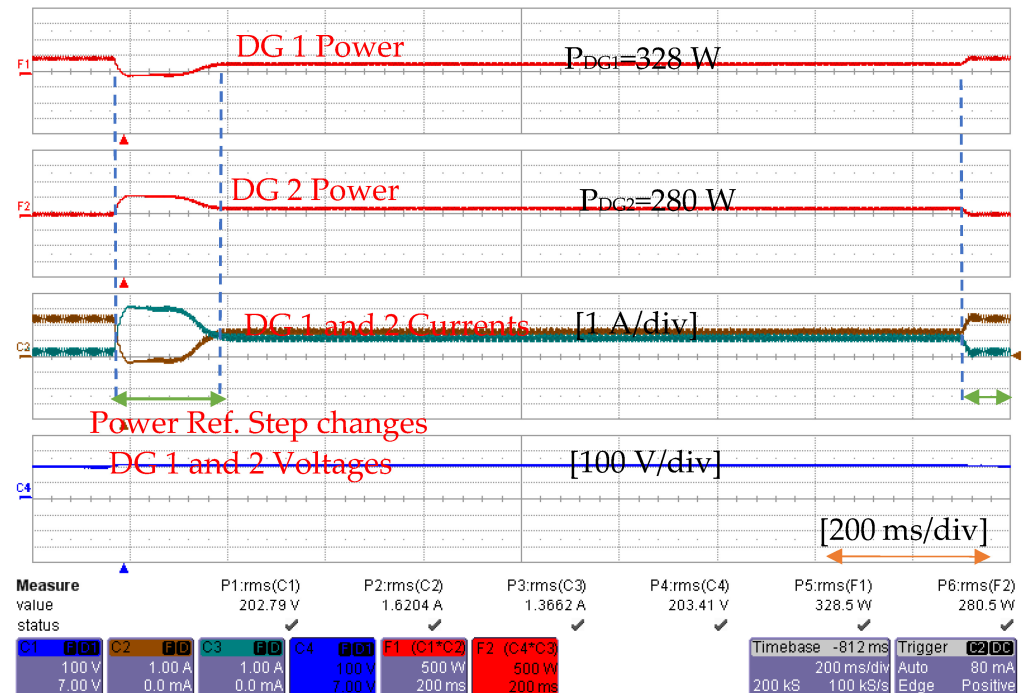


Figure 12. Dynamic response of DGs output parameters with the proposed SMC control.

Study II: Load Transfer

To assess the performance of the converters in a DC microgrid during a hot-swap operation, switches are connected at the output of the converters before the DC bus. These switches are operated to simulate the disconnection of the DG units due to an external fault.

During this test, the complete load is shifted to a single converter. Initially, a switch connected to DG 2 on the source side is operated to disconnect it from the MG network, transferring the load to DG 1. As depicted in Figure 13, the current of the DG 2 converter drops to zero, while the current of the DG 1 converter increases to accommodate the entire

load. Similarly, to swap the load to the DG 2 converter, a switch connected to DG 1 on the source side is operated, disconnecting DG #1. As observed in Figure 14, the DG 2 converter then supplies the full load.

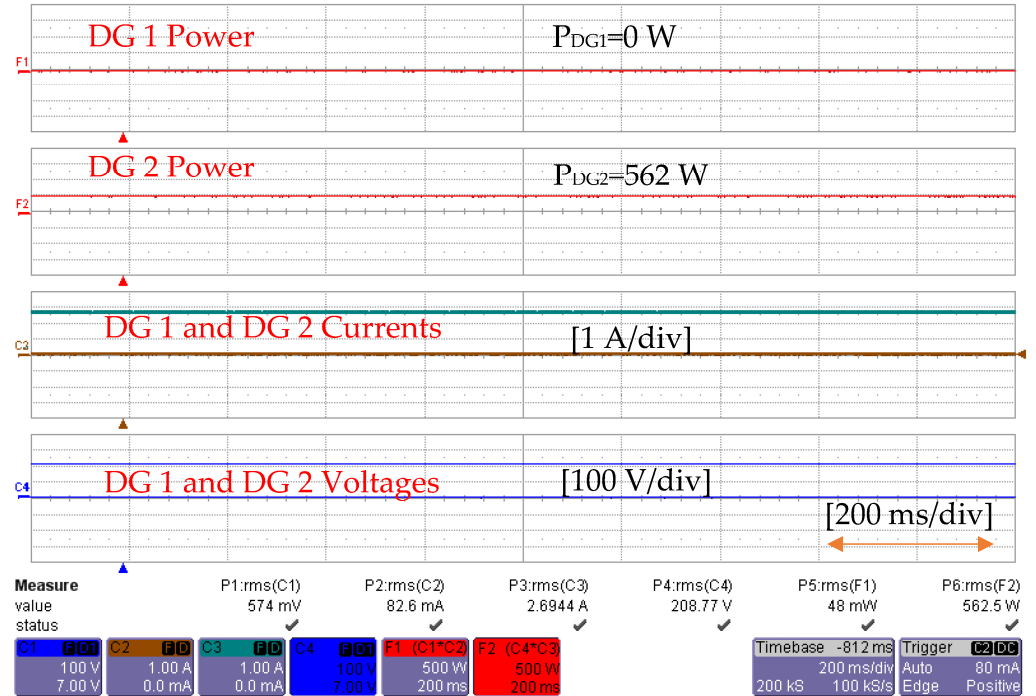


Figure 13. Hot-swap operation with full load on DG 2 and no load on DG 1.

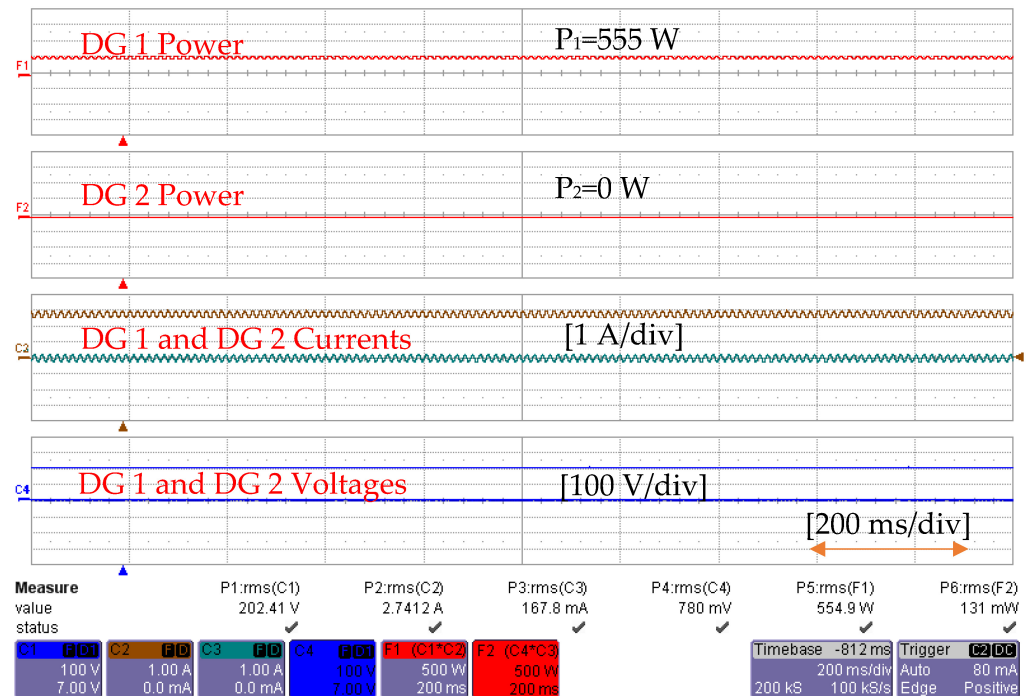


Figure 14. Hot-swap operation with no load on DG 2 and full load on DG 1.

Throughout these tests, the voltage across the output of the DGs remains regulated. During the hot-swap operation, the voltage and current exhibit stable behavior during the transition period. The converters within the microgrid network are designed to handle a fully connected load, ensuring their capability to handle such operations smoothly.

5. Conclusions

This paper focuses on the implementation of two control techniques, namely, sliding mode control (SMC) and proportional–integral (PI) control, for voltage stability and power sharing in DC microgrids. In order to enable efficient power sharing among the distributed generators (DGs), the proposed approach integrates universal droop control with SMC. By combining these control techniques, the system aims to achieve optimal voltage stability and effective power distribution among the DGs in the DC microgrid. The control signal for the switching of DC–DC boost converters in the microgrid network has been modeled using sliding mode control (SMC). The control signal in SMC has been defined to ensure Lyapunov stability. Initially, the proposed SMC control has been studied and analyzed for different operating conditions of the distributed generators (DGs) under various load scenarios. Subsequently, the integration of universal droop control with SMC has been implemented, enabling accurate power sharing between the DGs. Furthermore, for comparative analysis, the SMC control has been replaced with proportional–integral (PI) control. This allows for a comprehensive evaluation of the performance of the different control techniques in the microgrid system. The performance and effectiveness of both control types, sliding mode control (SMC) and proportional–integral (PI) control, have been thoroughly investigated in various scenarios, including step-change in load, load transfer, and hot-swap operation. The results demonstrate that the proposed SMC control exhibits superior performance compared to PI control. Additionally, the voltage regulation capabilities of both control types have been compared to determine the most suitable control strategy for a wide range of load variations. It is observed that SMC control outperforms PI control in terms of maximum load regulation while still achieving accurate power sharing between the distributed generators (DGs).

Author Contributions: Conceptualization, K.A.; methodology, K.A., I.H. and M.S.; software, K.A. and I.H.; validation, K.A., I.H. and M.S.; formal analysis, A.S. and S.M.; investigation, K.A.; resources, M.S.; writing—original draft preparation, K.A., I.H. and M.S.; writing—review and editing, M.S., S.M. and I.H.; visualization, K.A.; supervision, A.S.; project administration, M.S. and A.S. All authors have read and agreed to the published version of the manuscript.

Funding: This research received no external funding.

Data Availability Statement: Not Applicable.

Acknowledgments: The authors acknowledge the support provided by School of Science, Computing and Engineering Technologies and Swinburne University of Technology, Hawthorn, Australia and the Power Electronics and Renewable Energy Research Laboratory, Department of Electrical Engineering, University of Malaya, Kuala Lumpur 50603, Malaysia.

Conflicts of Interest: The authors declare no conflict of interest.

References

1. Hatziargyriou, N.; Dimeas, A.; Tsikalakis, A. Centralized and decentralized control of microgrids. *Int. J. Distrib. Energy Resour.* **2005**, *1*, 197–212.
2. Muhammad, R.; Muhammad, A.; Bhatti, A.I.; Minhas, D.M. Mathematical modeling and stability analysis of DC microgrid using SM hysteresis controller. *Int. J. Electr. Power Energy Syst.* **2018**, *95*, 507–522. [[CrossRef](#)]
3. Chang, F.; O'Donnell, J.; Su, W. Voltage Stability Assessment of AC/DC Hybrid Microgrid. *Energies* **2023**, *16*, 399. [[CrossRef](#)]
4. AlLee, G.; Tschudi, W. Edison redux: 380 Vdc brings reliability and efficiency to sustainable data centers. *IEEE Power Energy Mag.* **2012**, *10*, 50–59. [[CrossRef](#)]
5. Dragicevic, T.; Vasquez, J.C.; Guerrero, J.M.; Skrllec, D. Advanced LVDC Electrical Power Architectures and Microgrids: A step toward a new generation of power distribution networks. *IEEE Electr. Mag.* **2014**, *2*, 54–65. [[CrossRef](#)]
6. Liu, S.; Miao, H.; Li, J.; Yang, L. Voltage control and power sharing in DC Microgrids based on voltage-shifting and droop slope-adjusting strategy. *Electr. Power Syst. Res.* **2023**, *214*, 108814. [[CrossRef](#)]
7. Flourentzou, N.; Agelidis, V.G.; Demetriades, G.D. VSC-based HVDC power transmission systems: An overview. *IEEE Trans. Power Electron.* **2009**, *24*, 592–602. [[CrossRef](#)]
8. Cucuzzella, M.; Rosti, S.; Cavallo, A.; Ferrara, A. Decentralized sliding mode voltage control in DC microgrids. In Proceedings of the 2017 American Control Conference (ACC), Seattle, WA, USA, 24–26 May 2017; IEEE: Piscataway, NJ, USA, 2017; pp. 3445–3450.

9. Anand, S.; Fernandes, B.G.; Guerrero, J. Distributed control to ensure proportional load sharing and improve voltage regulation in low-voltage DC microgrids. *IEEE Trans. Power Electron.* **2012**, *28*, 1900–1913. [[CrossRef](#)]
10. Zhao, E.; Han, Y.; Zeng, H.; Li, L.; Yang, P.; Wang, C.; Zalhaf, A.S. Accurate Peer-to-Peer Hierarchical Control Method for Hybrid DC Microgrid Clusters. *Energies* **2022**, *16*, 421. [[CrossRef](#)]
11. Lu, X.; Guerrero, J.M.; Sun, K.; Vasquez, J.C. An improved droop control method for dc microgrids based on low bandwidth communication with dc bus voltage restoration and enhanced current sharing accuracy. *IEEE Trans. Power Electron.* **2013**, *29*, 1800–1812. [[CrossRef](#)]
12. Yang, N.; Paire, D.; Gao, F.; Miraoui, A.; Liu, W. Compensation of droop control using common load condition in DC microgrids to improve voltage regulation and load sharing. *Int. J. Electr. Power Energy Syst.* **2015**, *64*, 752–760. [[CrossRef](#)]
13. Mi, Y.; Guo, J.; Yu, S.; Cai, P.; Ji, L.; Wang, Y.; Yue, D.; Fu, Y.; Jin, C. A power sharing strategy for islanded DC microgrid with unmatched line impedance and local load. *Electr. Power Syst. Res.* **2021**, *192*, 106983. [[CrossRef](#)]
14. Cucuzzella, M.; Trip, S.; De Persis, C.; Cheng, X.; Ferrara, A.; van der Schaft, A. A robust consensus algorithm for current sharing and voltage regulation in DC microgrids. *IEEE Trans. Control Syst. Technol.* **2018**, *27*, 1583–1595. [[CrossRef](#)]
15. Guerrero, J.M.; Vasquez, J.C.; Matas, J.; De Vicuña, L.G.; Castilla, M. Hierarchical control of droop-controlled AC and DC microgrids—A general approach toward standardization. *IEEE Trans. Ind. Electron.* **2010**, *58*, 158–172. [[CrossRef](#)]
16. Hamzeh, M.; Ghazanfari, A.; Mohamed, Y.A.-R.I.; Karimi, Y. Modeling and design of an oscillatory current-sharing control strategy in DC microgrids. *IEEE Trans. Ind. Electron.* **2015**, *62*, 6647–6657. [[CrossRef](#)]
17. Liu, X.; Wang, P.; Loh, P.C. A hybrid AC/DC microgrid and its coordination control. *IEEE Trans. Smart Grid* **2011**, *2*, 278–286.
18. Tan, S.-C.; Lai, Y.-M.; Chi, K.T.; Martinez-Salamero, L.; Wu, C.-K. A fast-response sliding-mode controller for boost-type converters with a wide range of operating conditions. *IEEE Trans. Ind. Electron.* **2007**, *54*, 3276–3286. [[CrossRef](#)]
19. Tan, S.-C.; Lai, Y.; Tse, C.K.; Cheung, M.K. Adaptive feedforward and feedback control schemes for sliding mode controlled power converters. *IEEE Trans. Power Electron.* **2006**, *21*, 182–192.
20. Tan, S.-C.; Lai, Y.-M.; Chi, K.T. General design issues of sliding-mode controllers in DC–DC converters. *IEEE Trans. Ind. Electron.* **2008**, *55*, 1160–1174.
21. Fan, J.-C.; Kobayashi, T. A simple adaptive pi controller for linear systems with constant disturbances. *IEEE Trans. Autom. Control* **1998**, *43*, 733–736. [[CrossRef](#)]
22. Hussaini, H.; Yang, T.; Bai, G.; Urrutia-Ortiz, M.; Bozhko, S. Artificial Intelligence-Based Hierarchical Control Design for Current Sharing and Voltage Restoration in DC Microgrid of the More Electric Aircraft. *IEEE Trans. Transp. Electrif.* **2023**. [[CrossRef](#)]
23. Sabanovic, A.; Fridman, L.M.; Spurgeon, S.; Spurgeon, S.K. *Variable Structure Systems: From Principles to Implementation*; IET: London, UK, 2004; Volume 66.
24. Wai, R.-J.; Shih, L.-C. Design of voltage tracking control for DC–DC boost converter via total sliding-mode technique. *IEEE Trans. Ind. Electron.* **2010**, *58*, 2502–2511. [[CrossRef](#)]
25. Li, X.; Guo, L.; Zhang, S.; Wang, C.; Li, Y.W.; Chen, A.; Feng, Y. Observer-based DC voltage droop and current feed-forward control of a DC microgrid. *IEEE Trans. Smart. Grid* **2017**, *9*, 5207–5216. [[CrossRef](#)]
26. Meng, L.; Dragicevic, T.; Vasquez, J.; Guerrero, J.; Sanseverino, E.R. Hierarchical control with virtual resistance optimization for efficiency enhancement and State-of-Charge balancing in DC microgrids. In Proceedings of the 2015 IEEE First International Conference on DC Microgrids (ICDCM), Atlanta, GA, USA, 7–10 June 2015; pp. 1–6.
27. Li, F.; Lin, Z.; Xu, H.; Wang, F. Comprehensive local control design for eliminating line resistance effect on power sharing degradation in DC microgrids. *IET Power Electron.* **2022**, *15*, 11–22. [[CrossRef](#)]
28. Mohammed, N.; Callegaro, L.; Ciobotaru, M.; Guerrero, J.M. Accurate power sharing for islanded DC microgrids considering mismatched feeder resistances. *Appl. Energy* **2023**, *340*, 121060. [[CrossRef](#)]
29. Batiyah, S.; Sharma, R.; Abdelwahed, S.; Zohrabi, N. An MPC-based power management of standalone DC microgrid with energy storage. *Int. J. Electr. Power Energy Syst.* **2020**, *120*, 105949. [[CrossRef](#)]

Disclaimer/Publisher’s Note: The statements, opinions and data contained in all publications are solely those of the individual author(s) and contributor(s) and not of MDPI and/or the editor(s). MDPI and/or the editor(s) disclaim responsibility for any injury to people or property resulting from any ideas, methods, instructions or products referred to in the content.